

## Accepted Manuscript

Title: A facile approach to the synthesis of hydrophobic iron tetrasulfophthalocyanine (FeTSPc) nano-aggregates on multi-walled carbon nanotubes: A potential electrocatalyst for the detection of dopamine

Authors: Omobosede O. Fashedemi, Kenneth I. Ozoemena

PII: S0925-4005(11)00630-7  
DOI: doi:10.1016/j.snb.2011.06.085  
Reference: SNB 13253

To appear in: *Sensors and Actuators B*

Received date: 18-3-2011  
Revised date: 14-6-2011  
Accepted date: 30-6-2011

Please cite this article as: O.O. Fashedemi, K.I. Ozoemena, A facile approach to the synthesis of hydrophobic iron tetrasulfophthalocyanine (FeTSPc) nano-aggregates on multi-walled carbon nanotubes: A potential electrocatalyst for the detection of dopamine, *Sensors and Actuators B: Chemical* (2010), doi:10.1016/j.snb.2011.06.085

This is a PDF file of an unedited manuscript that has been accepted for publication. As a service to our customers we are providing this early version of the manuscript. The manuscript will undergo copyediting, typesetting, and review of the resulting proof before it is published in its final form. Please note that during the production process errors may be discovered which could affect the content, and all legal disclaimers that apply to the journal pertain.



**A facile approach to the synthesis of hydrophobic iron tetrasulfophthalocyanine (FeTSPc) nano-aggregates on multi-walled carbon nanotubes: A potential electrocatalyst for the detection of dopamine**

**Omobosedede O. Fashedemi<sup>1</sup> and Kenneth I. Ozoemena<sup>1,2,\*</sup>**

<sup>1</sup>*Department of Chemistry, University of Pretoria, Pretoria 0002, South Africa.*

<sup>1,2</sup>*Energy and Processes, Materials Science and Manufacturing, Council for Scientific & Industrial Research (CSIR), Pretoria 0001, South Africa.*

***Revised Manuscript to Sens Actuators B (Ms. Ref.: SNB-D-11-00393)***

---

\*Author to whom correspondence should be addressed:

Tel.: +27128413664; Fax: +27-12-8412135;

E-mail address: [kozoemena@csir.co.za](mailto:kozoemena@csir.co.za) (K.I. Ozoemena)

## Abstract

A facile method has been utilized to synthesize a hydrophobic form of nano-scaled iron (II) tetrasulfophthalocyanine (nanoFeTSPc), integrated with functionalized multi-walled carbon nanotubes (fMWCNT-nanoFeTSPc). The nanocomposite was characterized by UV-visible spectra, EDX, FESEM, and TEM. The electrocatalytic properties of the film on a glassy carbon electrode were investigated using cyclic voltammetry, electrochemical impedance spectroscopy, chronoamperometry and square wave voltammetry. The fMWCNT-nanoFeTSPc modified electrode demonstrated higher catalytic performance in terms of electron transport and current response compared to the other electrodes studied towards Dopamine (DA) detection giving a sensitivity of  $0.314 \mu\text{A } \mu\text{M}^{-1}$  and a limit of detection of  $9.86 \times 10^{-8} \text{ mol L}^{-1}$ . A selective detection was realized in elimination of ascorbic acid response on the film of fMWCNT-nanoFeTSPc. The detection limit in the presence of a high concentration of ascorbic acid was  $3.5 \times 10^{-7} \text{ mol L}^{-1}$ .

**Keywords:** Hydrophobic iron (II) tetrasulfophthalocyanine; MWCNTs; Electrocatalysis; Dopamine; Ascorbic Acid.

## 1. Introduction

Iron (II) tetrasulfophthalocyanine (FeTSPc, Figure 1) belongs to the N4-macrocyclic metal compounds related to the metalloporphyrins. Like every other sulfonated metallophthalocyanine (MTSPc) complex, FeTSPc is a highly water-soluble molecule and very well recognized for its unique physico-chemical properties and wide range of applications ranging from catalysis [1,2] to sensing [3,4] and photocatalysis [5-7]. The major handicap to the use of FeTSPc film in heterogeneous electrocatalysis is its high water-solubility [8-11]. The ease with which MTSPc complexes are washed away from electrodes during electrochemical studies has long been a major setback and has limited their fundamental studies and potential applications to heterogeneous electrocatalysis in aqueous environment. For example, the main problems usually associated with physical anchorage (such as drop-casting method) of FeTSPc films onto an electrode are poor stability (i.e., washing off into the aqueous electrolyte / analytical solution) as well as the difficulty in controlling the amount of film deposited. To curb the solubility problems, researchers have resorted to several techniques. For example, in 1992, Rusling's group [12] immobilized MTSPc (M = Fe, Cu, Ni) complexes by electrodepositing them from their aqueous solutions onto pyrolytic graphite electrode surface pre-modified with dioctadecyldimethylammonium salt (DODA). Since then, other workers have also used layer-by-layer self-assembly electrode modification strategy involving the use of polycationic and/or highly branched polymeric complexes such as polyamidoamine [13],

dendrimers [14], chitosan [15], and dimethylaminoethanethiol/carbon nanotubes [16]. These techniques are often laborious, use expensive and/or toxic reagents, and sometimes give semi-stable films. There is need therefore to explore means of making MTSPc complexes hydrophobic without compromising on their electrocatalytic activity towards the detection of analytes in aqueous conditions. Importantly, an ideal synthetic technique for such hydrophobic MTSPc should be easy to perform, produce large-surface area FeTSPc (nanostructures) for enhanced catalytic activity, and offer the possibility of mass production.

**(Figure 1)**

To our knowledge, nanostructured FeTSPc has never been reported, thus their electrocatalytic properties still remain unknown. The synthesis of hydrophobic MTSPc complexes is hugely limited [17], and neither their structural morphology nor their electrochemical properties were reported. In this work, we report the first synthesis of hydrophobic nanostructured FeTSPc complex assisted by hexadecyltrimethylammonium bromide (CTAB). Carbon nanotubes (CNTs) are known to enhance the electrocatalytic properties of metallophthalocyanine (MPc) complexes [18-22], thus in this work we also integrated nanostructured FeTSPc with multi-walled carbon nanotubes (MWCNTs) with a view to enhancing its electrocatalytic properties. We demonstrate that the nanostructured FeTSPc integrated with functionalized MWCNTs may be potentially useful as an efficient electrocatalyst for the detection of dopamine, a neurotransmitter, in the presence of high concentration of ascorbic acid.

## 2. Experimental

### 2.1 *Materials and reagents*

Tetra-sodium salt of sulfonic acid functionalised iron (II) phthalocyanine ( $\text{Na}_4[\text{FeTSPc}]$ ) (Fig. 1) was synthesized following the established procedure described elsewhere [8]. Hexadecyltrimethylammonium bromide ( $\text{C}_{16}\text{H}_{33}\text{N}^+(\text{CH}_3)_2\text{Br}^-$ , CTAB) was obtained from Merck. Multi-walled carbon nanotubes (MWCNTs, Sigma-Aldrich, purity > 90%, 110-170 nm in diameter, 5-9  $\mu\text{m}$  in length) were purified [23] and subsequently functionalized with sulfonic acid using the established procedure [24], abbreviated herein as fMWCNTs. Dopamine (4-(2-aminoethyl) benzene 1,2-diol) hydrochloride was purchased from Sigma-Aldrich. N, N-Dimethylformamide (DMF, Sigma-Aldrich) was distilled and dried before use. Ultra pure water of resistivity 18.2  $\text{M}\Omega\text{cm}$  was obtained from a Milli-Q Water System (Millipore Corp. Bedford, MA, USA) and was used throughout for the preparation of solutions.  $\text{KH}_2\text{PO}_4$  and  $\text{K}_2\text{HPO}_4$  were used to prepare phosphate buffer solutions (PBS) of the required pH. All electrochemical experiments were carried out in nitrogen atmosphere. All other reagents were of analytical grade and were used as received from the suppliers without further purification.

### 2.2 Preparation of nanoFeTSPc and fMWCNT-nanoFeTSPc

The procedure for the nanoFeTSPc was a modification of the previous work of using DODA for making organo-soluble metallophthalocyanines [17]. In a typical experiment, 123 g (0.34 mol) of CTAB was dissolved in 5 mL of

deionised water, then subjected to ultra sonication for about 1 h. 80g (0.08mol) of  $\text{Na}_4\text{FeTSPc}$  was dissolved in 2 ml  $10^{-3}$  M NaOH solution, both solutions were stirred with a magnetic stirrer at  $\sim 50$  °C for 2 h. The resulting hot paste-like crude product was dispersed with 20 mL warm water ( $\sim 40$  °C), suction-filtered and washed with copious amount of warm water several times, and finally with pentane. The dark-colored product is oven-dried at 70 °C, to obtain hydrophobic FeTSPc nanoparticles, abbreviated herein as nanoFeTSPc.

The nanoFeTSPc integrated with fMWCNTs was obtained as follows: In a typical experiment, 0.002g nanoFeTSPc was dissolved in 50 mL ethylene glycol in a 250 ml Erlenmeyer flask. 40 mg of functionalised-MWCNTs was then added into the above solution and ultrasonically dispersed in the solution for 1 h. The solution was then transferred into a liner-rotor 16 F100 TFM vessel, then placed in a microwave (Multiwave 3000 sample preparation system, 1400 Watts, Anton Paar) and heated using 1000 Watts at 190 °C for 60 s. The resulting suspension was separated by filtration and the obtained residue washed with acetone and deionised water. The final product, abbreviated herein as fMWCNT-nanoFeTSPc, was dried at 110 °C overnight in an oven. For comparison, the functionalised MWCNT was mixed with the nanoFeTSPc in ethylene glycol, ultrasonicated, and dried as above. The mixed product is abbreviated herein as fMWCNT-nanoFeTSPC<sub>(mix)</sub>.

### 2.3 Apparatus and procedure

The UV-visible spectra were recorded using a Cary 300 UV-Visible Spectrophotometer, driven by Varian software version 3.0. Transmission electron microscopy (TEM) experiment was carried out using a Model JEOL JEM 2100F field emission transmission (FESEM) images were obtained from JEOL JSM 5800 LV (Japan). The energy dispersive X-ray spectra (EDX) were obtained using NORAN VANTAGE (USA). All electrochemical experiments were carried out using an Autolab Potentiostat PGSTAT 100 (Eco Chemie, Utrecht, The Netherlands) driven by version 4.9 of GPES and FRA softwares). The working electrode was a modified glassy carbon disk electrode (GCE, Bioanalytical systems, diameter = 3.0 mm). A Pt rod and Ag|AgCl (saturated 3 M KCl) were used as a counter and reference electrode, respectively. Electrochemical impedance spectroscopy (EIS) measurements were performed with Autolab Frequency Response Analyzer (FRA) software between 100 kHz and 10 mHz with the amplitude (rms value) of the ac signal of 10 mV. All solutions were de-aerated by bubbling pure nitrogen prior to each electrochemical experiment. All experiments were performed at room temperature.

### 2.4 Electrode modification

Prior to the experiments, the bare GCE was first cleaned using slurries of aluminum oxide nano-powder (Sigma-Aldrich), mirror finished on a Buehler felt pad and then subjected to ultrasonic vibration in ethanol and acetone to remove residual alumina nano-powder at the surface. The drop cast



technique was utilized for the modification of the electrode. 1 mg nanoFeTSPc was dispersed in 1 mL Ethanol containing 100  $\mu$ L 5% Nafion and ultrasonicated for some minutes. Thereafter, 10  $\mu$ L was dropped on the electrode, and allowed to dry in an oven at 80  $^{\circ}$ C. The electrode obtained is abbreviated as GCE-nanoFeTSPc. The above procedure was adopted for making electrodes containing the MWCNTs alone (i.e., GCE-fMWCNT), and the microwave-synthesized MWCNT-nanoFeTSPc alone (i.e., GCE-fMWCNT-nanoFeTSPc) as well as the mixture of fMWCNT and nanoFeTSPc, i.e., GCE-fMWCNT-nanoFeTSPC<sub>(mix)</sub>.

### **3. Results and Discussion**

#### **3.1 UV-Vis, SEM, TEM and EDX characterisation**

Unlike the highly hydrophilic FeTSPc, the nanoFeTSPc complex is hydrophobic, soluble in organic solvents such as the DMF, DMSO and ethanol. As will be seen from the following discussion, the preparation protocol adopted in this work led to changes in the physico-chemical properties of the nanoFeTSPc complex. Figure 2 shows the comparative UV-visible spectra for the FeTSPc, nanoFeTSPc and MWCNT-nanoFeTSPc in DMF. The observed spectra exhibited the characteristic Q-band typical of monomeric species of metallophthalocyanine complexes. There is no detectable difference between the spectra of the FeTSPc and nanoFeTSPc, which is an indication that the synthetic protocol adopted here did not impact on the structural properties of the FeTSPc. The FeTSPc and nanoFeTSPc show

the characteristic absorption bands at 350 nm (B-band) and 685 nm (Q-band). The weak band at about 430 nm is typical of a low-spin six-coordinate Fe(II)Pc species and are usually associated with Fe(II)-to-ligand transfer transition [25,26]. Hence its presence is a good indication that the central metal ion remains in the +2 oxidation state.

**(Figure 2)**

Figure 3 compares the FESEM images of fMWCNT-nanoFeTSPc(mix) (a) and fMWCNT-nanoFeTSPc (b). Evidently, nanoFeTSPc show a tendency to have a strong interaction with the fMWCNTs (Figure 3b) compared with the direct mixing of nanoFeTSPc with fMWCNTs (Figure 3a). The size of the nanoFeTSPc is not uniform, it varies between 20 and 60 nm. EDX spot analysis provided semi-quantitative information on elemental concentrations of the FeTSPc at different locations in the film. For example, a typical atomic percent gave the following result: S  $24.95 \pm 0.23\%$  and Fe  $5.85 \pm 0.22\%$ , which is the expected atomic ratio of Fe:4S, suggesting that the 4 sulfonate groups of the FeTSPc molecule are associated with the ammonium head groups of the CTAB via ionic exchange reaction. The EDX result also gave trace amount of Br ( $\sim 7\%$ ) impurity from CTAB.

**(Figure 3)**

### **3.2 Cyclic voltammetry at electrode-immobilized Films**

Figure 4 is a comparative cyclic voltammetric evolutions of the GCE-immobilized films of (i) fMWCNT, (ii) nanoFeTSPc (iii) fMWCNT-nanoFeTSPc,

(iv) fMWCNT-nanoFeTSPc<sub>(mix)</sub> and (v) bare GCE in 0.01 M PBS (pH 7.0) at 50 mVs<sup>-1</sup>.

**(Figure 4)**

The voltammetric parameters in terms of the ratio of the anodic to cathodic peak current heights ( $I_{pa}/I_{pc}$ ), peak-to-peak separation potential ( $\Delta E_p$ ), and the half-peak potential ( $E_{1/2}$ ) are summarized in Table 1.

**(Table 1)**

The results suggest electrochemical reversibility, and the presence of MWCNTs. Unlike the bare GCE, all the modified films showed well-defined redox process (**I**) around the 0.15 V region. This redox process for the nanoFeTSPc is attributed to the Fe(II)/Fe(III) redox couple. The two redox processes of the fMWCNT (**I** and **II**) are due to the presence of the phenolic/quinolic species on the edge-plane sites of the MWCNTs. Thus, the well-defined redox process of the fMWCNT-nanoFeTSPc is multi-electron process arising from the combined redox processes of the fMWCNT and Fe(II)/Fe(III). Also, the microwave-synthesized fMWCNT-nanoFeTSPc seems to show better redox process than its "mixed" counterpart, possibly due to the close association of the nanoFeTSPc with the fMWCNTs (see FESEM images). Also note that the capacitive currents (at the  $\leq 0.1$  V and  $\geq 0.35$  V regions) of the MWCNT-nanoFeTSPc is about twice smaller than observed at either the MWCNT-nanoFeTSPc<sub>(mix)</sub> or the nanoFeTSPc alone. The voltammetric responses shown in Figure 4 were repeatable, and showed no

significant change in current heights during continuous cycling, indicating electrochemical stability.

### **3.3 Electrocatalytic detection of dopamine**

Figure 5 compares the cyclic voltammetric evolutions of the GCE-immobilised films of (i) fMWCNT, (ii) nanoFeTSPc (iii) fMWCNT-nanoFeTSPc, (iv) fMWCNT-nanoFeTSPc(mix) and (v) bare GCE in 0.01 M PBS (pH 7.0) containing  $10^{-4}$  M dopamine.

#### **(Figure 5)**

The voltammetric parameters (i.e.,  $I_{pa}$ ,  $I_{pc}$ ,  $I_{pa}/I_{pc}$ ,  $\Delta E_p$ , and  $E_{1/2}$ ) are summarized in Table 2. The fMWCNT-nanoFeTSPc and fMWCNT-nanoFeTSPc(mix) gave the best reversibility, but the fMWCNT-nanoFeTSPc showed the highest dopamine detection current.

#### **(Table 2)**

The better electrochemical response exhibited by the fMWCNT-nanoFeTSPc film compared to the other films is ascribed to the combined activities nanoparticulate nature of the MWCNTs and the FeTSPc, easy diffusion of dopamine through the larger surface area of the film, the possibility of electrostatic interaction between the negatively-charged fMWCNTs and the positively-charged DA (DA is positively charged at pH 7.4 or in neutral environment [27]). There are notable differences between the voltammograms obtained in the buffer alone (Figure 4) and in solution containing DA (Figure 5). For example, the current response of the DA at the

fMWCNT-nanoFeTSPc is very huge ( $I_{pa}$  or  $I_{pc} \approx 15 \mu\text{A}$ ) compared to the very small current at the buffer ( $I_{pa}$  or  $I_{pc} \approx 1 \mu\text{A}$ ) (see Figure 5 inset). Also, importantly, the redox peaks of DA occurred approximately at the same positions of the redox couple of fMWCNT and Fe(II)/Fe(III) seen in the buffer solution alone. These observations clearly confirm that the voltammetric response of the DA is catalytically mediated by the redox processes of fMWCNT-nanoFeTSPc modified electrode.

Further insights into the electrocatalytic detection of DA were obtained using the electrochemical impedance spectroscopy (EIS). Figure 6 shows typical impedance spectra (Nyquist plots) obtained at the GCE-immobilised films of (i) fMWCNT, (ii) nanoFeTSPc (iii) fMWCNT-nanoFeTSPc, and (iv) fMWCNT-nanoFeTSPc<sub>(mix)</sub> at the equilibrium potential of  $\sim 0.18 \text{ V}$  vs. Ag|AgCl sat'd KCl.

### (Figure 6)

The experimental data were satisfactorily fitted with the modified Randles electrical equivalent circuit (Fig 6 inset) which incorporates the constant phase element (CPE), the solution resistance ( $R_s$ ), charge transfer resistance ( $R_{ct}$ ), and Warburg impedance ( $Z_w$ ) relating to the semi-infinite linear diffusion process. These values are summarized in Table 3. The most important parameter,  $R_{ct}$ , is lowest at the MWCNT-nanoFeTSPc, indicating the higher catalytic properties of this film, and corroborating the CV data. Thus, all other studies carried out in this work, unless otherwise stated, were focused on MWCNT-nanoFeTSPc electrode.

### (Table 3)

Effect of scan rate ( $\nu$ ) was investigated by carrying out cyclic voltammetry experiment at constant concentration ( $10^{-4}$  M) of the DA in 0.01 M PBS (pH 7.0) using the fMWCNT-nanoFeTSPc electrode (Fig. 7a). Fig 7b is the plot of peak current versus square root of scan rate, showing that the DA anodic and cathodic peaks increase simultaneously with increase in scan rates (scan rates ranging from 25–1000  $\text{mV s}^{-1}$ ). The linearity of the plot is an indication that the electrochemical interaction between the MWCNT-nanoFeTSPc electrode and DA is diffusion-controlled. The plots of peak current,  $I_p$  for both anodic and cathodic versus square root of scan rate ( $\nu^{1/2}$ ) (Fig. 6b) were linear ( $R^2 = 0.9956$  and  $0.9939$ ), signifying a diffusion-controlled redox process. During this study, the electrode maintained stable voltammograms when repeated at each scan rate, proving its usability in aqueous solution.

**(Figure 7)**

To determine the diffusion coefficient ( $D$ ) of DA on this film, chronoamperometric study was carried out by setting the operating condition at a potential of 0.2 V vs Ag|AgCl sat'd KCl. The diffusion coefficient was estimated from the Cottrell Equation (1):

$$I = \frac{nFAD^{1/2}C}{\pi^{1/2}t^{1/2}} \quad (1)$$

where  $C$  is the bulk concentration ( $\text{mol cm}^{-3}$ ),  $A$  is the area of the electrode in  $\text{cm}^2$  and assuming  $n \approx 2$  [28], from the experimental plots of  $I$  versus  $t^{-1/2}$  at different concentrations (not shown), the diffusion coefficient  $D$  of DA was calculated as  $(5.65 \pm 0.23) \times 10^{-5} \text{ cm}^2 \text{ s}^{-1}$ . The  $D$  value is higher compared to

some other electrodes reported in the literature [29-32], indicating that this film permits faster DA diffusion.

### 3.4 Concentration study

Figure 8 shows square wave voltammetric current responses at two different concentration ranges of DA; (0.0 to 5.6  $\mu\text{M}$ , Fig 8a) and (0.0 to 5.36  $\mu\text{M}$ , Fig 8b).

#### (Figure 8)

From the plot of current response against concentration (insets in Fig. 8), linear relationships were obtained for the two concentration ranges; 0.0 to 6.0  $\mu\text{M}$  (equation 2) and 0.0 to 54  $\mu\text{M}$  (equation 3):

$$I_p / \mu\text{A} = (0.310 \pm 0.003) [\text{DA}] / \mu\text{M} + (200 \pm 1) \times 10^{-8} \quad (R^2 = 0.9985) \quad (2)$$

$$I_p / \mu\text{A} = (0.379 \pm 0.004) [\text{DA}] / \mu\text{M} + (30 \pm 1.53) \times 10^{-7} \quad (R^2 = 0.9984) \quad (3)$$

The values of sensitivity ( $0.379 \pm 0.004$ )  $\mu\text{A}/\mu\text{M}$  and limit of detection ( $\text{LoD} = 3 s/m$  [33], where  $s$  is the relative standard deviation of the intercept, and  $m$  the slope of the linear current versus the concentration of DA) are summarized in Table 3. The LoD lower, than many other electrodes reported in literature (Table 4) for DA electrocatalysis and detection [34-44].

#### (Table 4)

### 3.5 Interference study

Ascorbic acid is the major interferent to DA in physiological fluids. Figure 9 shows SWV current response of DA concentrations in 0.01 M PBS (pH 7.0) solution containing  $10^{-2}$  M AA. Note that the peak potential of DA showed a negative shift ( $\sim 90$  mV) compared to its original peak potential of  $\sim 200$  mV. At the neutral pH used in this study, AA is negatively-charged while the DA is positively-charged [49]. Thus, this observed substantial negative shift in potential in the presence of AA is related to the electrostatic interaction between the negatively-charged AA with the positively-charged DA. The linear relationship between the DA peak current and concentration is:

$$I_p/\mu\text{A} = (0.36 \pm 0.001)[\text{DA}] / \mu\text{M} + (658 \pm 4) \times 10^{-8} \quad (R^2 = 0.9999) \quad (4)$$

Indeed, there is no major difference between this SWV result with high concentration of AA and the data obtained in the absence of AA (Figure 8b) since the sensitivity and LoD of DA are essentially the same. This is very interesting considering that an efficient DA sensor is expected to detect DA in physiological solution at Millimolar Concentration of AA.

### (Figure 9)

## Conclusions

Hydrophobic nanoparticles of FeTSPc, integrated with MWCNTs, have been synthesized and characterized for the detection of dopamine. The MWCNT-nanoFeTSPc based electrode showed stable and reproducible



voltammograms (CV and SWV) for the detection of DA. The fMWCNT-nanoFeTSPc modified electrode could satisfactorily detect dopamine even at very low concentrations in the presence of excess interfering ascorbic acid at physiological conditions. The proposed technique of making hydrophobic nanoFeTSPc is simple and could open new doors of making related metallophthalocyanine complexes for application as electrocatalysts for the detection and analysis of several analytes.

### **Acknowledgments**

We thank NRF and CSIR for supporting this work. Omobosedede O. Fashedemi thanks NRF/DST "National Nanotechnology flagship" for PhD bursary.

## References

1. D. Ji, X. Lu and R. He, Syntheses of cyclic carbonates from carbon dioxide and epoxides with metal phthalocyanines as catalyst. *Appl. Catal., A: General* 203, (2000) 329-333.
2. K.Ozoemena, and T.Nyokong, Octabutylthiophthalocyaninatoiron(II): electrochemical properties and interaction with cyanide. *J. Chem. Soc., Dalton Trans.*, 2002, 1806–1811.
3. S. Griveau, M.Gulppi, J.Pavez, J-H.Zagal, F.Bedioui, Cobalt Phthalocyanine-Based Molecular Materials for the Electrocatalysis and Electroanalysis of 2-Mercaptoethanol, 2-Mercaptoethanesulfonic Acid, Reduced Glutathione and L-Cysteine. *Electroanalysis* 15 (2003) 779-785.
4. A.W. Snow and W.R. Barger in Phthalocyanines: properties and applications, eds, C.C. Leznoff and A.B.P. Lever, VCH Publishers, New York, 1989, Vol 1. Ch.5.
5. W.H Flora, H. K. Hall, and N. R. Armstrong, Guest Emission Processes in Doped Organic Light-Emitting Diodes: Use of Phthalocyanine and Naphthalocyanine Near-IR Dopants. *J. Phys. Chem. B.* 107 (2003) 1142-1150.
6. K. Ozoemena, N. Kuznetsova and T. Nyokong, "Comparative photosensitized transformation of polychlorophenols with different sulfonated metallophthalocyanine complexes in aqueous medium", *J. Mol. Catal. A: Chem.* 176 (2001) 29-40.
7. B. Agboola, K.I. Ozoemena, and T. Nyokong, Comparative efficiency of immobilized non-transition metal phthalocyanine photosensitizers for the visible light transformation of chlorophenols. *J. Mol. Catal. A: Chem.* 248 (2006) 84–92.
8. Weber J.H, Busch D.H. *Inorg. Chem.* 4 (1965) 469 -471.
9. M. Pirouzman, M.M. Amini, N. Safari. Immobilization of iron tetrasulfophthalocyanine on functionalized MCM-48 and MCM-41 mesoporous silicas: Catalysts for oxidation of styrene. *J. Colloid Interface Sci.* 319 (2008) 199-205.
10. J. Oni and T. Nyokong. Interaction between iron(II) tetrasulfophthalocyanine and the neurotransmitters, serotonin and dopamine. *Polyhedron* 19 (2000) 1355-1361.

11. N. Li, M. Zhu, M. Qu, X. Gao, X. Li, W. Zhang, J. Zhang, J. Ye .Iron-tetrasulfophthalocyanine functionalized graphene nanosheets: Attractive hybrid nanomaterials for electrocatalysis and electroanalysis. *J. Electroanal. Chem.* 651 (2011) 12-18.
12. N.Hu, D.J. Howe, M.F. Ahmadi, and J. F. Rusling. Stable Films of Cationic Surfactants and Phthalocyaninetetrasulfonate Catalysts. *Ana. Chem.* 64 (1992) 3180-3188.
13. J. R. Siqueira Jr., F. N. Crespilho, V. Zucolotto, O. N. Oliveira Jr. Bifunctional electroactive nanostructured membranes. *Electrochem. Commun.* 9 (2007) 2676–2680.
14. J. R. Siqueira Jr.,L. H. S. Gasparotto, O. N. Oliveira, Jr.,and V. Zucolotto. Processing of Electroactive Nanostructured Films Incorporating Carbon Nanotubes and Phthalocyanines for Sensing. *J. Phys. Chem. C*, 112 (2008) 9050–9055.
15. A. B. Sorokin , F. Quignard R.Valentin,S. Mangematin. Chitosan supported phthalocyanine complexes: Bifunctional catalysts with basic and oxidation active sites. *Appl. Catal. A: General* 309 (2006) 162–168.
16. J.F. Silva, S. Griveau, C. Richard, J.H. Zagal, F.Bedioui, Glassy carbon electrodes modified with single walled carbon nanotubes and cobalt phthalocyanine and nickel tetrasulphonated phthalocyanine: Highly stable new hybrids with enhanced electrocatalytic performances. *Electrochem. Commun.* 9 (2007) 1629–1634.
17. M. Sanchez, E.Fache, D. Bonnet, B. Meunier. Synthesis of Organo-soluble metallophthalocynines bearing electron withdrawing substituents. *J. Porphyrins Phthalocyanines* 5 (2001) 867-872.
18. T. Mugadza, T. Nyokong. Covalent linking of ethylene amine functionalized single-walled carbon nanotubes to cobalt (II) tetracarboxyl-phthalocyanines for use in electrocatalysis. *Synth. Met.* 160 (2010) 2089–2098.
19. S.A. Mamuru, K.I. Ozoemena, T. Fukudac, N. Kobayashic, T.Nyokong. Studies on the heterogeneous electron transport and oxygen reduction reaction at metal (Co, Fe) ctabutylsulphonylphthalocyanines supported on multi-walled carbon nanotube modified graphite electrode. *Electrochim. Acta* 55 (2010) 6367–6375.
20. K. Wu, J. Fei, and S. Hu. Simultaneous determination of dopamine and serotonin on a glassy carbon electrode coated with a film of carbon nanotubes. *Anal. Biochem.* 318 (2003) 100–106.

21. B. O. Agboola, J. Pillay, K. Makgopa and K.I. Ozoemena. Electrochemical Characterisation of mixed self Assembled films of water-soluble single walled carbon nanotube – Poly(m-aminobenzene sulfonic acid) and Iron (II) tetrasulfophthalocyanine. *J. Electrochem. Soc.* 157(2010) 159-166.
22. Y. Wang, H-Z. Chen, H-Y Li, M. Wang. Fabrication of carbon nanotubes/copper phthalocyanine composites with improved compatibility. *Mater. Sci. Eng. B* 117 (2005) 296–301.
23. M. P. Siswana, K.I. Ozoemena, T.Nyokong. Electrocatalysis of asulam on cobalt phthalocyanine modified multi-walled carbon nanotubes immobilized on a basal plane pyrolytic graphite electrode. *Electrochim. Acta* 52 (2006) 114–122.
24. Z-P. Sun, X-G. Zhang, Y-Yu. Liang, Hu-Lin Li. A facile approach towards sulfonate functionalization of multi-walled carbon nanotubes as Pd catalyst support for ethylene glycol electro-oxidation . *J. Power Sources* 191 (2009) 366–370.
25. A. B. P. Lever, R. Pickens, P. C. Minor, S. Licoccia, B. S. Ramaswamy, and K. Magnell . Charge-Transfer Spectra of Metallophthalocyanines: Correlation with Electrode Potentials. *J. Am. Chem. Soc.* 103 (1981) 6800-6806.
26. T. Nyokong and M.J. Stillman in Phthalocyanines : Properties and Applications eds. C.C. Leznoff and A.B.P. Lever, VCH Publishers, New York, 1989, Vol. 1.
27. Teresa Łuczak .Preparation and characterization of the dopamine film electrochemically deposited on a gold template and its applications for dopamine sensing in aqueous solution. *Electrochim. Acta* 53 (2008) 5725–5731.
28. A.J. Bard, L.R. Faulkner, *Electrochemical Methods*, John Wiley and Sons, New York, 2001.
29. G. Gerhardt and R. N. Adams. Determination of Diffusion Coefficients by Flow Injection Analysis. *Anal. Chem.* 54 (1982) 2618-2620.
30. Guo-Song Lai, Hai-Li Zhang, De-Yan Han. Electrocatalytic oxidation and voltammetric determination of dopamine at a Nafion carbon-coated iron nanoparticles-chitosan composite film modified electrode. *Microchim. Acta* 160 (2008) 233–239.

31. W.Song, Yu Chen, J. Xu, D. Bi Tian. A selective voltammetric detection for dopamine using poly (gallic acid) film modified electrode. *Chin. Chem. Lett.* 21 (2010) 349–352
32. E. A. Khudaish, M.R. Al Birikei. The role of bromine adlayer at palladium electrode in the electrochemical oxidation of dopamine in alkaline solution. *J. Electroanal. Chem.* 650 (2010) 68–74.
33. G.D. Christian, *Analytical Chemistry*, 6<sup>th</sup> Edition . John Wiley and Sons. New York.2004,p113.
34. P-Y chen,R.Vittal,P Nien,K-C. Ho, Enhancing dopamine detection using glassy carbon electrode modified with MWCNTs, quercetin, and Nafion, *Biosen. Bioelectron.* 24 (2009) 3504-3509.
35. D.Zheng, J.Ye, W.Zhang, Some properties of Sodium Dodecyl sulfate functionalized multiwalled carbon nanotubes electrode and its application on the detection of Dopamine in the presence of Ascorbic Acid. *Electroanalysis* 20 (2008) 1811- 1817.
36. S.Shahrokhian, H.R. Mehrjardi. Electrochemical Synthesis of Polypyrrole in the presence of Congo red; Application to selective Voltammetric Determination of Dopamine in the presence of Ascorbic Acid. *Electroanalysis* 21 (2009) 157-164.
37. A.S. Adekunle, B.O.Agboola, J.Pillay, K.I.Ozoemena. Electrocatalytic detection of dopamine at single walled carbon nanotubes-iron (III) oxide nanoparticles Platform. *Sens. Actuators, B.* 148 (2010)93-102.
38. S. Shahrokhian, H.R. Mehrjardi. Cobalt salophen-modified carbon paste incorporating a cationic surfactant for simultaneous voltammetric detection of ascorbic acid and dopamine. *Sens. Actuators, B* 121(2007)530-537.
39. C.C. Harley, A.D. Rooney, C.B. Breslin . The selective detection of Dopamine at a polypyrrole film doped with sulfonated  $\beta$ -cyclodextrins. *Sens. Actuators, B.* 150 (2010) 498-504.
40. Z.Zhu,L.Qu,Y Guo,Y Zeng,W Sun,X Huang. Electrochemical Detection of Dopamine on a Ni/Al layered double hydroxide modified carbon ionic liquid electrode. *Sens. Actuators, B.* 151 (2010) 146- 152.
41. J. Ping, J.Wu, Y. Ying, Development of an ionic liquid modified screen – printed graphite electrode and its sensing in determination of dopamine. *Electrochem. Commun.* (2010) 121738–1741.

42. S. Thiagarajan, S.-M. Chen, Preparation and characterization of PtAu hybrid film modified electrodes and their use in simultaneous determination of dopamine, ascorbic acid and uric acid. *Talanta* 74 (2007) 212–222.
43. M. Koshki, E. Shams, Selective response of dopamine in the presence of ascorbic acid on carbon paste electrode modified with titanium phosphated silica gel. *Anal. Chim. Acta* 587 (2007) 110-115.
44. J.Oni, P. Westbroek, T. Nyokong, Electrochemical Behaviour and detection of Dopamine and Ascorbic Acid at Iron (II) tetrasulfophthalocyanine modified Carbon paste Microelectrode. *Electroanalysis* 15 (2003) 847-854.
45. P.R. Roy, T. Okajima, T. Ohsaka, Simultaneous electroanalysis of dopamine and ascorbic acid using poly(N,N-dimethylaniline)-modified electrodes. *Bioelectrochem.* 59 (2003) 11 – 19.

## List of Tables and Figures

**Table 1:** Cyclic Voltammetric parameters obtained for the modified electrodes in 0.1M pH 7.0 PBS solution at scan rate of 50mVs<sup>-1</sup>.

**Table 2:** Cyclic Voltammetric parameters obtained for the modified electrodes in 10<sup>-4</sup>M DA in 0.1M pH 7.0 PBS solution at scan rate of 25mVs<sup>-1</sup>.

**Table 3:** Impedance data obtained for the modified GCE in 10<sup>-4</sup>M DA in 0.1MPBS (pH7) solution at 0.17V (vs Ag/AgCl sat'd KCl).

**Table 4:** Comparison of analytical performances of different modified Electrodes

**Figure 1:** (a) Molecular structures of sodium salt of iron (II) tetrasulphophthalocyanine (FeTSPc) complex.

**Figure 2:** UV-Visible Spectra of FeTSPc and nanoFeTSPc in DMF solution

**Figure 3:** FESEM images of (a) fMWCNT-nanoFeTSPC<sub>mix</sub> and (b) fMWCNT-nanoFeTSPc.

**Figure 4:** Comparative cyclic voltammetric evolutions of the modified electrodes in 0.1 M PBS (pH7.0) at 50 mVs<sup>-1</sup>.

**Figure 5:** Typical cyclic voltammograms of GCE-fMWCNT-nanoFeTSPc, GCE-fMWCNT-nanoFeTSPC<sub>mix</sub>, GCE-fMWCNT, GCE-nanoFeTSPc and Bare GCE in 0.1 M PBS (pH 7.0) containing 10<sup>-4</sup> M DA at scan rate of 25 mVs<sup>-1</sup>. Inset compares the expanded versions of the voltammograms obtained at GCE-fMWCNT-nanoFeTSPc (i) and Bare GCE (ii).

**Figure 6:** Typical Nyquist plots obtained for the modified electrodes in  $10^{-4}$ M dopamine in 0.1M PBS (pH 7.0) solution at a fixed potential 0.17 V (vs Ag/AgCl,sat'dKCl), inset is circuit used in the fitting of the Electrochemical Impedance data.

**Figure 7:** Cyclic voltammetric evolutions of GCE-MWCNT-nanoFeTSPc obtained in 0.1 M PBS (pH 7.0) containing  $10^{-4}$  M DA at scan rates 25-1200  $\text{mVs}^{-1}$ . Inset is the plot of current ( $I_p$ ) vs square root of scan rate.

**Figure 8:** (a) Square wave voltammetric evolutions of GCE-MWCNT-nanoFeTSPc in 0.1 M PBS (pH 7.0) solution containing increasing concentrations of DA (0, 0.33, 0.99, 1.32, 1.64, 2.28, 2.60, 3.32, 4.15, 4.46, 4.76, 5.06, 5.36, 5.66  $\mu\text{M}$ ) and (b) (0, 3.32, 6.62, 9.90, 13.2, 16.4, 19.6, 22.8, 26.0, 32.3, 38.5, 47.6, 50.6, 53.6  $\mu\text{M}$ ).

**Figure 9:** Typical square wave voltammetric responses of GCE-MWCNT-nanoFeTSPc in 0.1 M PBS (pH 7.0) solution containing increasing concentrations of DA (0, 2.6, 5.9, 8.9, 11.8, 17.6, 20.5, 23.3, 26.19, 34.5, 40.1, 45.6, and 51.0)  $\mu\text{M}$  with  $10^{-2}$ M AA. Inset is the plot showing linear relationship between DA peak current and concentration.



**Table 1:** Cyclic Voltammetric parameters obtained for the modified electrodes in 0.1 M PBS (pH 7.0) solution at scan rate of 50 mVs<sup>-1</sup>.

GCE modifiers	Cyclic voltammetric parameter						
	$E_{pa}$ (mV)	$E_{pc}$ (mV)	$\Delta E_p$ (mV)	$E_{p1/2}$ (mV)	$I_{pa}$ ( $\mu$ A)	$I_{pc}$ ( $\mu$ A)	$I_{pa}/I_{pc}$
fMWCNT	228	53	117.5	640	0.619	0.935	0.66
NanoFeTSPc	244	56	118	150	0.069	0.078	0.88
fMWCNT-nanoFeTSPc <sub>mix</sub>	213	144	69	179	0.094	0.081	1.16
fMWCNT-nanoFeTSPc	211	138	73	175	1.140	1.120	1.02

**Table 2:** Cyclic Voltammetric parameters obtained for the modified electrodes in  $10^{-4}$  M DA in 0.1 M PBS (pH 7.0) solution at scan rate of  $25\text{mVs}^{-1}$ .

GCE modifiers	Cyclic voltammetric parameter						
	$E_{pa}$ (mV)	$E_{pc}$ (mV)	$\Delta E_p$ (mV)	$E_{p\frac{1}{2}}$ (mV)	$I_{pa}$ ( $\mu\text{A}$ )	$I_{pc}$ ( $\mu\text{A}$ )	$I_{pa}/I_{pc}$
fMWCNT	225	119	106	172	9.60	9.80	0.92
NanoFeTSPc	279	115	164	197	3.20	2.93	1.10
fMWCNT-nanoFeTSPc <sub>mix</sub>	223	146	77	184.5	7.60	5.90	1.30
fMWCNT-nanoFeTSPc	212	142	70	177	14.90	14.7	1.01

**Table 3:** Impedance data obtained for the modified BGE electrodes in  $10^{-4}$  M DA in 0.1 M PBS (pH7.0) solution at 0.17 V (vs Ag/AgCl sat'd KCl). All values were obtained from the fitted impedance spectra after several iterations using the circuit in Figure 6 . Note that the values in parenthesis are the estimated percentage errors in fitting the experimental impedance spectra.

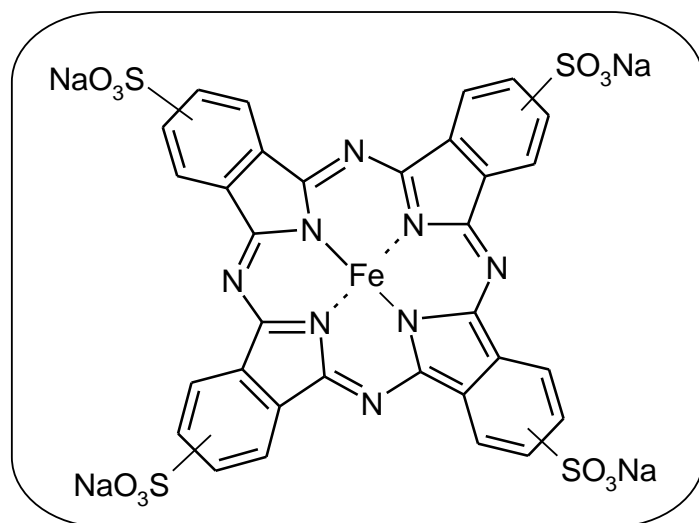
Electrode	Electrochemical Impedance Spectral Parameters				
	$R_s / \Omega$	CPE / $\mu\text{F}$	n	$R_{ct} / \text{k}\Omega$	$10^4 Z_w / \Omega\text{s}^{-1/2}$
fMWCNT	141.30 (1.14)	3.75 (2.81)	0.85 (0.48)	7.89 (1.34)	1.81 (3.16)
NanoFeTSPc	133.20 (1.80)	1.47 (3.04)	0.87 (0.48)	17.0 (1.53)	0.88 (3.90)
fMWCNT-nanoFeTSPc <sub>mix</sub>	135.10 (0.99)	2.57 (3.20)	0.89 (0.50)	4.09 (1.51)	0.97 (1.30)
fMWCNT-nanoFeTSPc	130.40 (1.61)	3.31 (5.40)	0.88 (0.84)	3.41 (2.20)	1.65 (2.41)

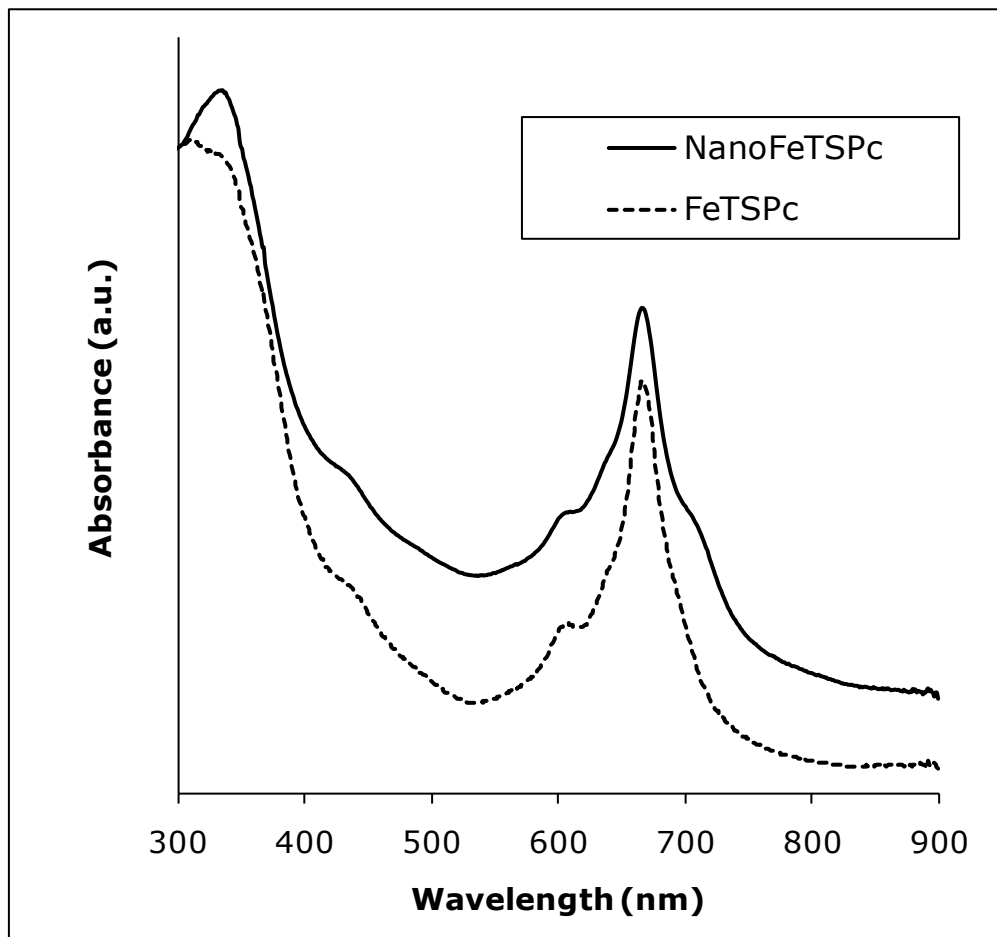
**Table 4:** Comparative voltammetric response of dopamine at various electrodes

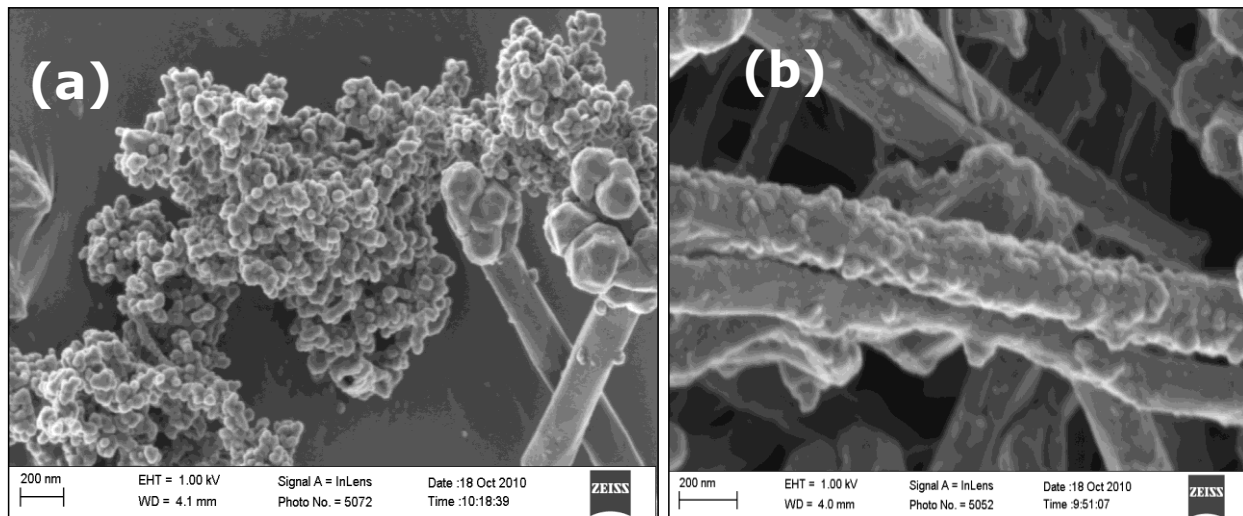
<b>Electrode</b>	<b>Conditions</b>	<b>Detection Method</b>	<b>Linear range (<math>\mu\text{M}</math>)</b>	<b>LoD (<math>\mu\text{M}</math>)</b>	<b>Ref</b>
MWCNT/Q/Nafion modified GC	PBS (pH7.0)	Chronoamp (FIS)	1.4- 300	1.4	34
SDS-MWCNT-modified GC	PBS (pH5.5)	DPV	20-200	3.75	35
PPy-CR-modified GC	PBS (pH 5.0)	DPV	0.5-100	0.1	36
SWCNT-Fe <sub>2</sub> O <sub>3</sub> modified EPPG	PBS (pH 7.0)	SWV	3.2-31.8	0.36	37
CoNSal/TOAB modified CP	Acetate Buffer (pH5.0)	DPV	1-100	0.7	38
PPY doped sulphonated $\beta$ -cyclodextrin modified Pt	CPB (pH 6.0)	CV	-	3.2	39
LDH modified CILE	PBS (pH 7.0)	DPV	10-1100	5.0	40
G-CA-OPPF screen printed electrode	PBS (pH 7.0)	DPV	1-2500	0.5	41

Pt/Au -L- cystein hybrid modified GC	KHP (pH 4.0)	DPV	24-384	5.0	42
Si-TiPH modified CP	PBS(pH 7.5)	DPV	2-60	0.043	43
FeTSPc modified CPME	PBS(pH 7.4)	CV	-	0.45	44
MWCNT-nanoFeTSPc modified GC	PBS (pH 7.0)	SWV	0 - 60	0.098	This work
MWCNT-nanoFeTSPc modified GC	PBS (pH 7.0)	SWV	20 - 51	0.35	This work

MWCNT: Multiwalled carbon nanotubes, Q: Quercetin, GC : Glassy Carbon, CPB : Citrate Phosphate Buffer , PPY : Polypyrrole, Pt : Platinum, FIS: Flow injection System, LDH: Ni/Al layered double hydroxide, CILE: carbon ionic liquid Electrode, Si-TiPH: Titanium phosphate grafted on silica gel, CP: Carbon paste, FeTSPc- Tetrasulfo Iron Phthalocyanine, CR: Congo red, CoNSAI: Cobalt - 5- nitrosalophene, TOAB : Tetraoctylammoniumbromide, SDS : Sodium duodecylsulfate, G-CA: Graphite cellulose Acetate, OPPF: n-octylpyridinum hexafluorophosphate., SWCNT: Single walled carbon nanotubes, Fe<sub>2</sub>O<sub>3</sub> : Iron (II) oxide, KHP: Potassium hydrogen phosphate , CPME : Carbon paste micro electrode.

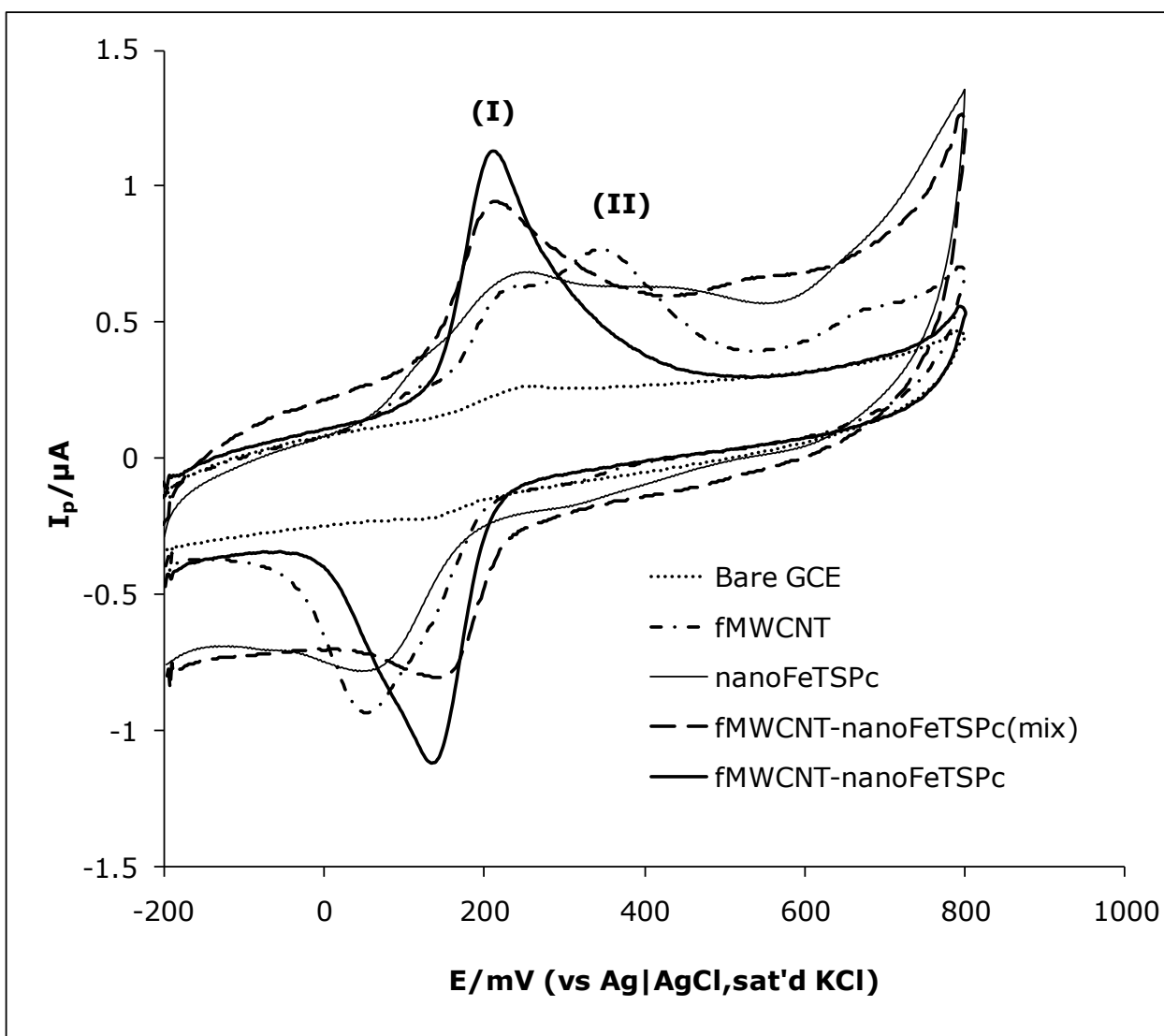
**Figure 1**

**Figure 2**



**Figure 3:**



**Figure 4**

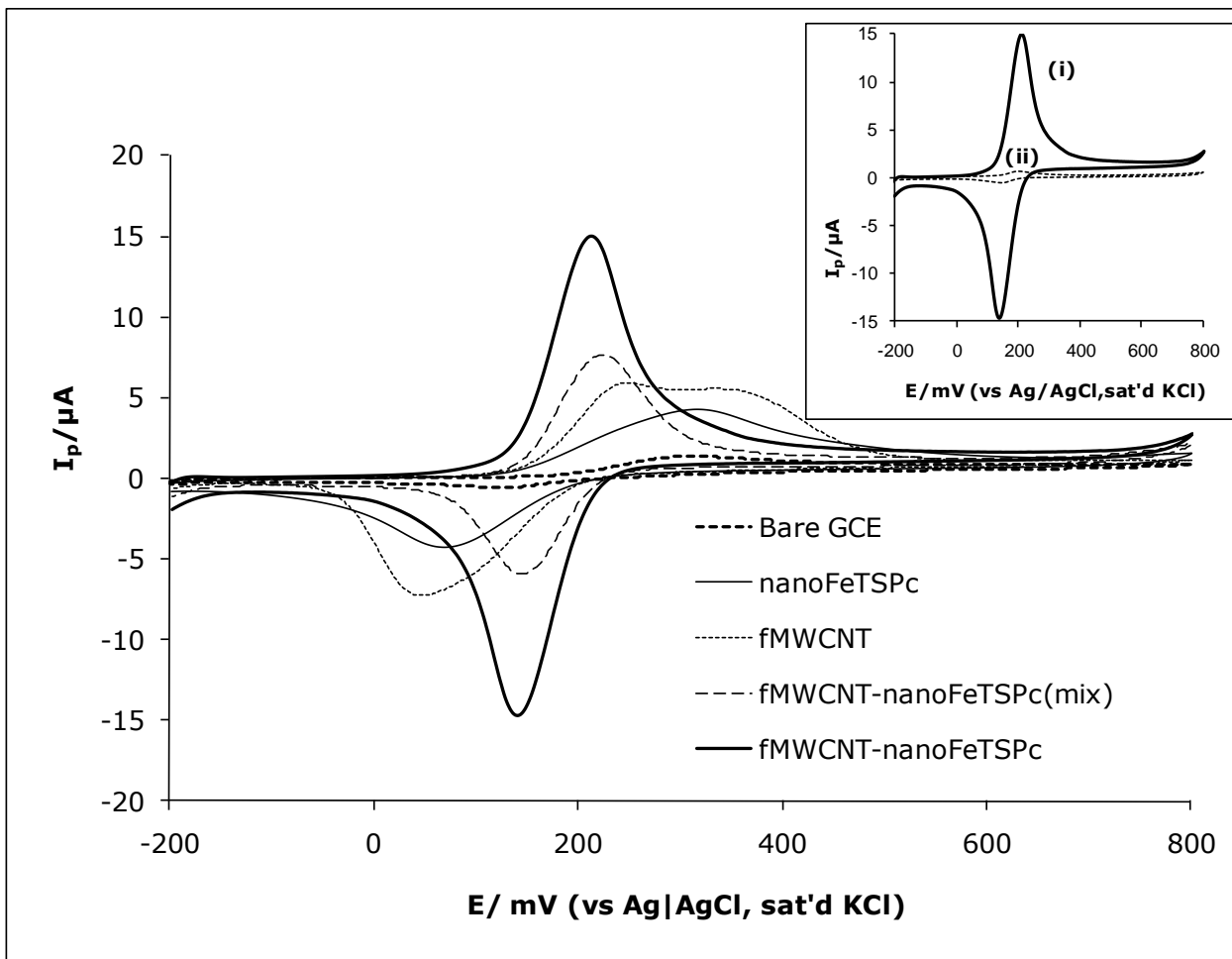


Figure 5

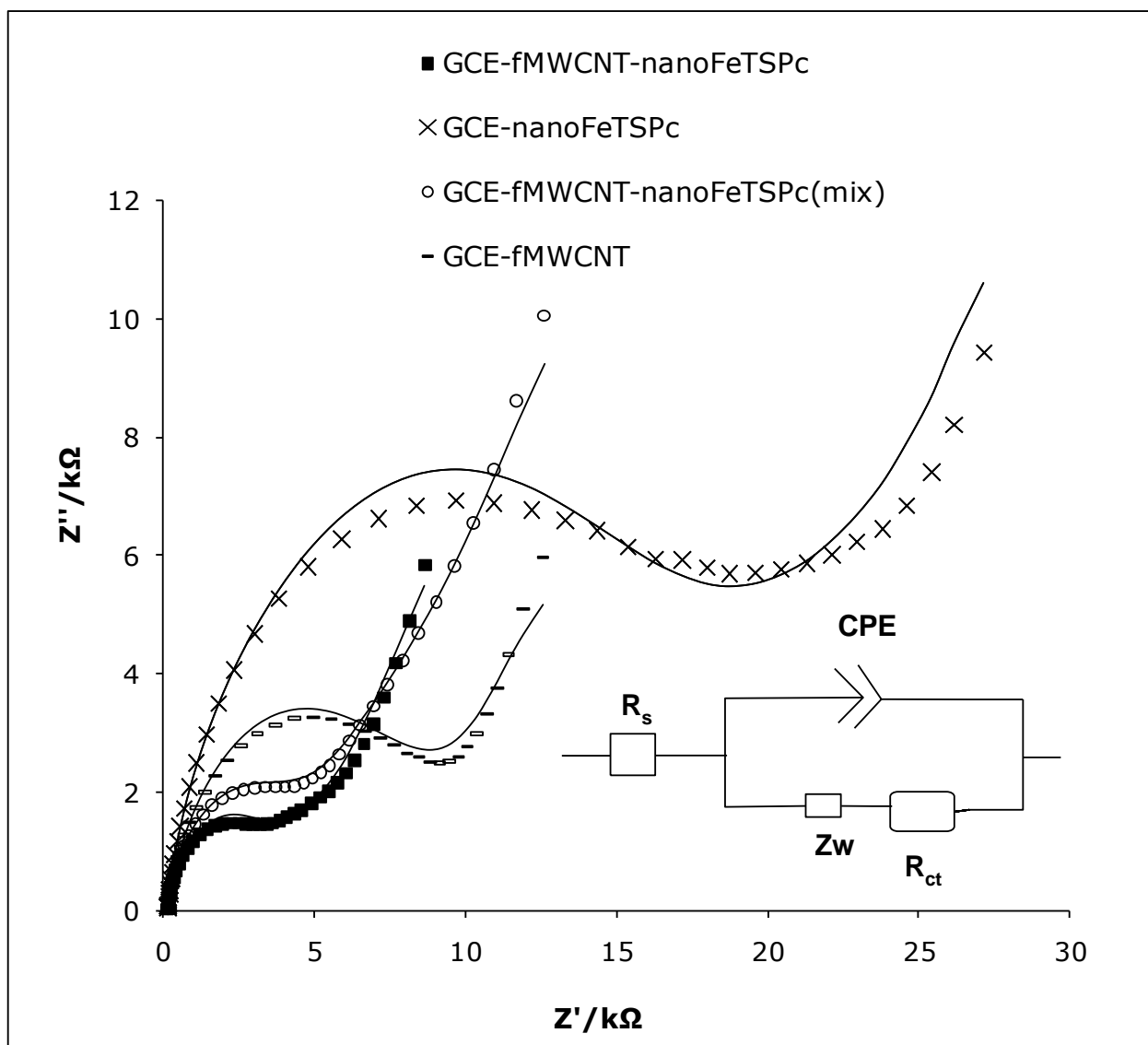
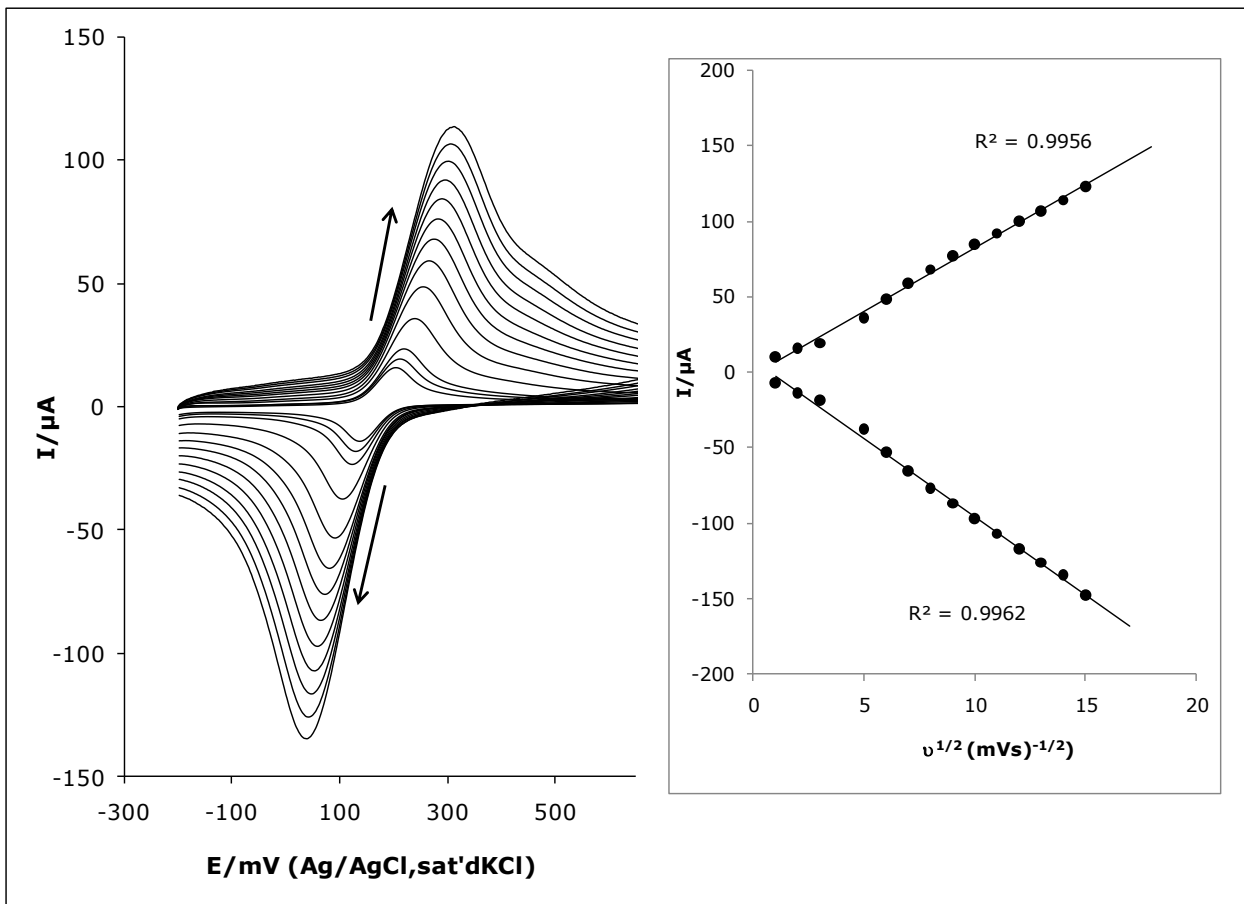


Figure 6

**Figure 7**

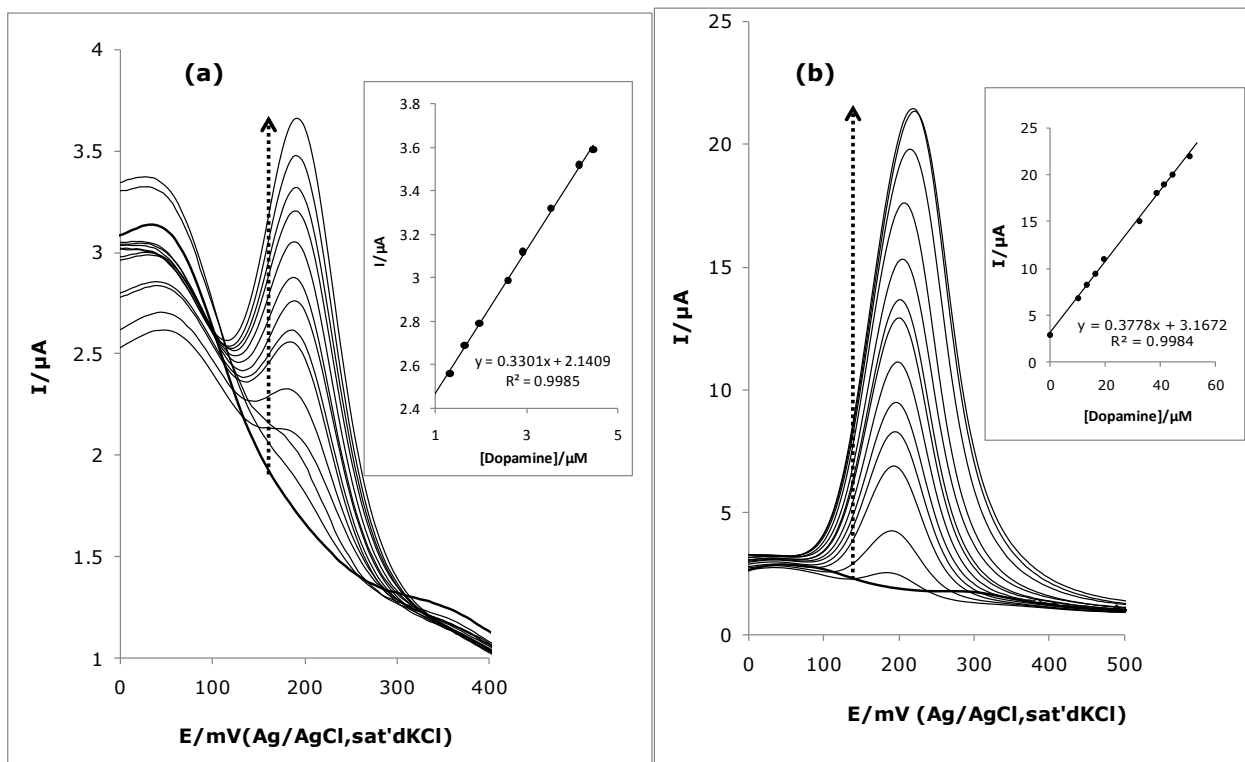


Figure 8

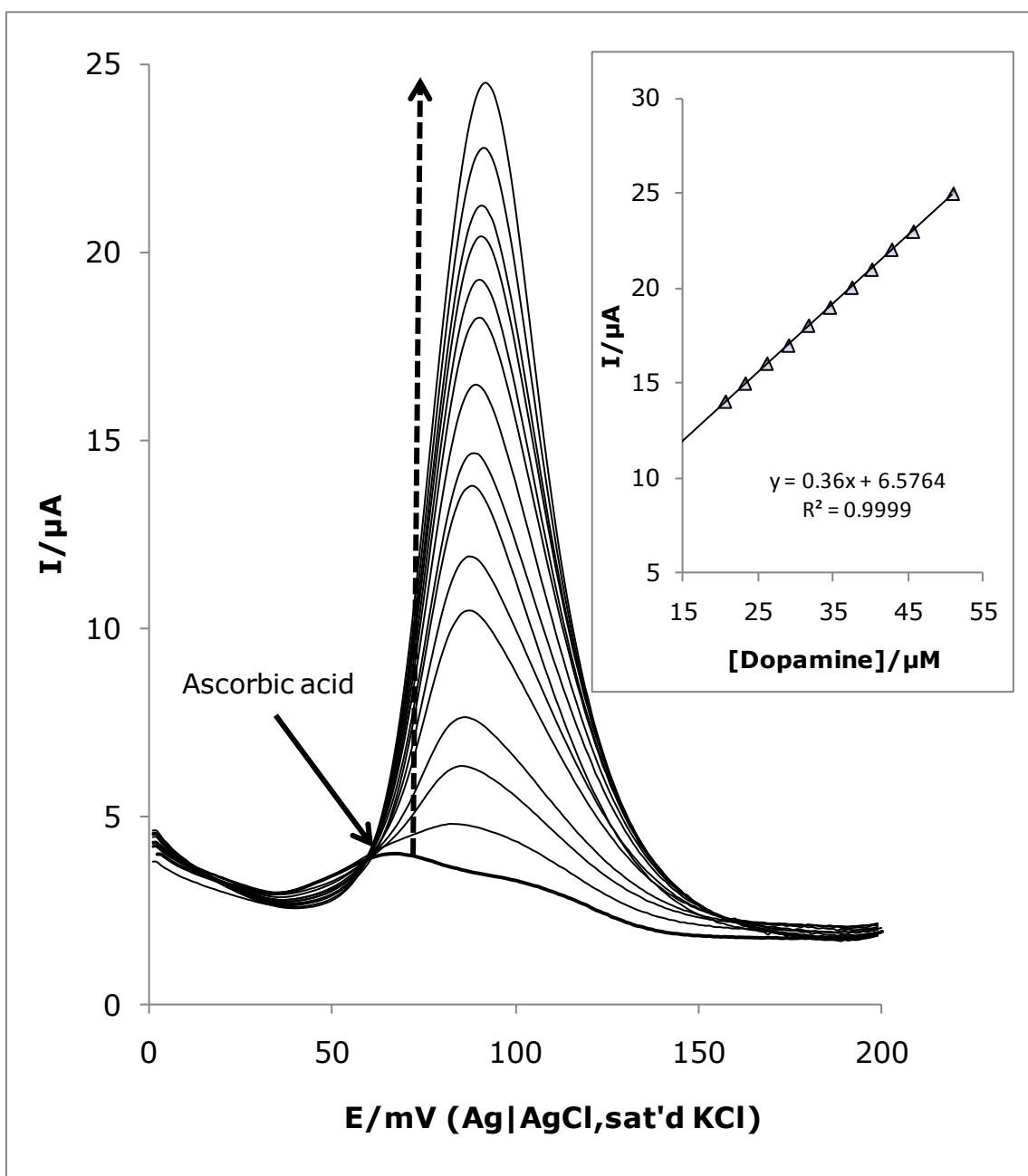


Figure 9